



compressibility effects separately or simultaneously. Rarefaction takes place by either the size or pressure of a fluid system decreases resulting in a mean free path of the fluid molecules that is comparable to the characteristic length of the system itself. In such cases, discontinuities between the fluid and the solid surface, as well as other noncontinuum behavior begin to develop. The very first parameters that are affected by rarefaction are velocity slip and temperature jump. Further Kn number, the ratio of mean free path to the length characteristics of the flow, increases in the fluid systems cause requirement of higher order and more sophisticated models for shear stress and heat flow.

Navier-stokes-based fluid dynamics solvers are often inaccurate when applied to Micro Electro Mechanical Device (MEMS). This inaccuracy stems from the calculation of molecular transport effects, such as viscous dissipation and thermal condition, from bulk flow quantities, such as mean velocity and temperature. The approximation of microscale phenomena using macroscale information fails as the characteristic length of the gaseous flow gradients ( $l$ ) approaches the average distance traveled by molecules between collisions.

Four different flow regims are observed based on the value of the Knudsen number, continuum flow for  $Kn \leq 0.001$ ; slip flow regime for  $0.001 \leq Kn \leq 0.1$ ; transition regime for  $0.1 \leq Kn \leq 10$  and free molecular regime for  $Kn \geq 10$  (Beskok and Kardianakis (1994) ). Kn determines the degree of rarefaction and the degree of the validity of the continuum approach. As Kn increases, rarefaction effects become more important, and eventually the continuum approach breaks down. Palm (2001), Sobhan and Garimella (2001) and Obot (2002) reviewed the experimental results in the existing literature for the convective heat transfer in microchannels. Morini (2004) presents an excellent review of the experimental data for convective heat transfer in microchannels. Barron et al. (1996) and Barron et al. (1996) extended the Graetz problem to slip-flow and developed simplified relationships to describe the effect of slip-flow on the convection heat transfer coefficient. Ameal et al. (1997) analytically treated the problem of laminar gas flow in micro tubes with a constant heat flux boundary condition at the wall assuming a slip flow hydrodynamic condition and a temperature jump thermal condition at the wall. They found that the fully developed Nusselt number decreased with Knudsen number. Tunc and Bayazitoglu (2001) investigated steady laminar hydrodynamically developed flow in microtubes with uniform temperature and uniform heat flux boundary conditions using the integral technique. They included temperature jump condition at the wall and viscous heating within the medium. Aydin and Aydin and Avci (2001) studied laminar forced convective heat transfer of a Newtonian fluid in a microchannel between two parallel plate analytically. Sparrow and Line (1962) examined laminar heat transfer in microtubes under slip-flow conditions and Inman (1964) investigated laminar slip-flow heat transfer in a parallel-plate channel with uniform wall heating and cartesian a formula for calculation of Nusselt number in this condition. Also Hadjicostantinou and Simek (2002) investigated the constant-wall-temperature convection heat transfer

characteristics of a model gaseous flow in two-dimensional micro and nano-channels under hydrodynamically and thermally fully developed conditions. They covered both the slip flow regime and most of the transition regime. Their results shown that the slip flow prediction is in good agreement with the DSMC results for  $Kn \leq 0.1$ . They also show that the Nusselt number decreases monotonically with increasing Knudsen number in a fully accommodating case, both in slip flow and transition regimes.

The aim of the present study is to present a new method for modeling the slip velocity and temperature jump in slip flow regime. For this purpose we numerically investigate rarefied gas flow in a microchannel between two parallel plates. Both the CWHF and CWT thermal boundary conditions are applied at the wall. The governing equations are solved in conjunction with the velocity slip and temperature jump to account for rarefaction effects in slip flow regime. Three-term perturbation expansions of velocity, pressure and temperature are used for developing of governing equations. The equations with different orders of Knudsen number are obtained. These equations are solved using SIMPLE algorithm. We compare Poiseuille number and Nusselt number with the results obtained by others.

## 2. PROBLEM DESCRIPTION

The computations are performed a micro-channel with constant heat flux (CWHF) and constant wall temperature (CWT) boundary conditions. We investigate hydrodynamically and thermally developing, steady state, laminar, incompressible two-dimensional flow with constant properties. The flow of gas is considered through two horizontal parallel-plates of length  $L$  that are a distance  $H$  apart and a cartesian coordinate system as shown in Fig. 1. The effects of compressibility and viscous dissipation are neglected due to low speed flows associated with micro-channel. A Channel length ( $L$ ) is chosen much larger than its height to ensure the thermally and hydrodynamically fully developed flow condition at the channel exists. As shown in Fig. 1, the velocity and temperature profiles are uniform at inlet of the channel and are based on  $Re = 1$ . For constant and uniform heat flux boundary condition, Nitrogen is used with constant properties. For constant-wall temperature (CWT) boundary condition, air with constant properties is selected as the working fluid in the channel. Also we assumed  $\lambda$ , is constant so Knudsen number varies by changing  $H$ .

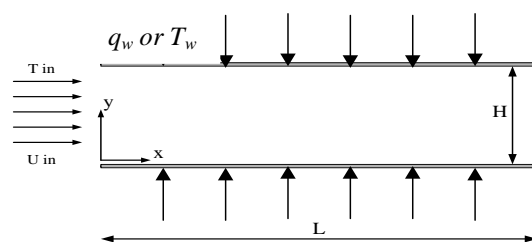


Fig. 1. Channel geometry

### 3. PERTURBATION METHOD and NUMERICAL SOLUTION

The macroscopic properties  $\varphi$  of the flow may be written with an asymptotic expansions as a function of the Knudsen number (Karniadakis and Beskok (2004) and Qin *et al.* (2007)):

$$\begin{aligned} \varphi &= \varphi_0 + Kn\varphi_1 + Kn^2\varphi_2 + Kn^3\varphi_3 + \dots \\ \varphi &= u, v, w, P, T, \rho, \dots \end{aligned} \quad (1)$$

Where  $\varphi_0$  corresponds to the no-slip flow,  $\varphi_1, \varphi_2, \varphi_3$  are the first, second and third order corrections of the  $\varphi_0$  respectively. Increase of the Knudsen number, i.e. going from slip to free molecular flow regime, higher corrections of the  $\varphi$  become important. In the slip flow regime we can use Navier-Stokes equations with use appropriate velocity slip and temperature jump conditions (Karniadakis and Beskok (2004)).

In this paper, a new method for modeling of microflows is introduced. Governing equations are developed by using perturbation expansions of velocity, pressure and temperature fields. Subsequently, different orders of equations depending on the value of Knudsen number are obtained. These set of equations are discretized in two-dimensional state on a staggered grid using finite volume method. In this study three-term perturbation expansions are used. These equations are obtained for up to second order magnitude respect to  $Kn$ . Total algorithm of solution includes three steps and solved with the SIMPLE algorithm.

Many second-order models have been proposed either experimentally or numerically and some have proven useful in increasing the range and accuracy of the slip boundary condition representation of rarefaction. There is currently insufficient experimental data to validate the use of any particular second-order model. Presently, however, there are few analytical or numerical convective heat transfer solutions based on second-order slip boundary condition models, and these are often presented for limited values of Knudsen number, momentum and thermal accommodation coefficients, geometry and consequently have limited applicability.

In this research we use three-term expansions and substitute these expansions into momentum and energy equations and boundary conditions, Momentum and energy equations are described as:

$$\begin{aligned} \nabla \cdot \vec{V} &= 0 \\ \rho \frac{D\vec{V}}{Dt} &= -\nabla p + \mu \nabla^2 \vec{V} \\ \rho C_p \frac{DT}{Dt} &= k \nabla^2 T \end{aligned} \quad (2)$$

Perturbation expansions of velocity ( $\vec{V} = u\hat{i} + v\hat{j}$ ), pressure and temperature fields are defined by (Karniadakis and Beskok (2004)):

$$\begin{aligned} u &= u_0 + Kn u_1 + Kn^2 u_2 + \dots \\ v &= v_0 + Kn v_1 + Kn^2 v_2 + \dots \\ P &= P_0 + Kn P_1 + Kn^2 P_2 + \dots \\ T &= T_0 + Kn T_1 + Kn^2 T_2 + \dots \end{aligned} \quad (3)$$

By substituting these expansions in Momentum and energy equations, One can reach to three-order of

equations  $O(1)$ ,  $O(Kn)$ ,  $O(Kn^2)$  and their boundary conditions, therefore for the zeroth-order equations and their boundary conditions, we have:

$$\begin{aligned} \rho \left[ \frac{\partial \vec{V}_0}{\partial t} + (\vec{V}_0 \cdot \nabla) \vec{V}_0 \right] &= -\nabla P_0 + \mu \nabla^2 \vec{V}_0 \\ \frac{\partial T_0}{\partial t} + \nabla \cdot (T_0 \vec{V}_0) &= \alpha \nabla^2 T_0 \end{aligned} \quad (4)$$

In fact the above equations are the no-slip Navier-Stokes and energy equations. The zeroth-order boundary conditions on the wall are defined as:

$$\begin{aligned} U_0|_s &= U_w \\ T_0|_s &= T_w \end{aligned} \quad (5)$$

Where  $U_0 = u_0/u_m$  and  $u_m$  is mean stream wise velocity. The first order  $O(Kn)$  equations and their boundary conditions on the walls are described by:

$$\begin{aligned} \rho \left[ \frac{\partial \vec{V}_1}{\partial t} + (\vec{V}_1 \cdot \nabla) \vec{V}_0 + (\vec{V}_0 \cdot \nabla) \vec{V}_1 \right] &= -\nabla P_1 + \mu \nabla^2 \vec{V}_1 \\ \frac{\partial T_1}{\partial t} + \nabla \cdot (T_0 \vec{V}_1) + \nabla \cdot (T_1 \vec{V}_0) &= \alpha \nabla^2 T_1 \end{aligned} \quad (6)$$

$$\begin{aligned} U_1|_s &= \frac{2 - \sigma_v}{\sigma_v} \left( \frac{\partial U_0}{\partial n} \right) |_s \\ T_1|_s &= \frac{2 - \sigma_T}{\sigma_T} \left[ \frac{2\gamma}{\gamma + 1} \right] \frac{1}{Pr} \left( \frac{\partial T_0}{\partial n} \right) |_s \end{aligned} \quad (7)$$

Where  $U_1 = u_1/u_m$ . Finally the second order equations  $O(Kn^2)$  are presented as:

$$\begin{aligned} \frac{\partial \vec{V}_2}{\partial t} + (\vec{V}_0 \cdot \nabla) \vec{V}_2 + (\vec{V}_2 \cdot \nabla) \vec{V}_0 + (\vec{V}_1 \cdot \nabla) \vec{V}_1 &= -\nabla P_2 + \mu \nabla^2 \vec{V}_2 \\ \frac{\partial T_2}{\partial t} + \nabla \cdot (T_0 \vec{V}_2) + \nabla \cdot (T_2 \vec{V}_0) + \nabla \cdot (T_1 \vec{V}_1) &+ \nabla \cdot (T_0 U_1) = \alpha \nabla^2 T_2 \end{aligned} \quad (8)$$

And the boundary conditions for  $O(Kn^2)$  are defined as:

$$\begin{aligned} U_2|_s &= \frac{2 - \sigma_v}{\sigma_v} \left[ \frac{\partial U_1}{\partial n} + \frac{1}{2} \frac{\partial^2 U_0}{\partial n^2} \right] \\ T_2|_s &= \frac{2 - \sigma_T}{\sigma_T} \left[ \frac{2\gamma}{\gamma + 1} \right] \frac{1}{Pr} \left[ \frac{\partial T_1}{\partial n} + \frac{1}{2} \frac{\partial^2 T_0}{\partial n^2} \right] \end{aligned} \quad (9)$$

Where  $U_2 = u_2/u_m$ . Also the first and second order equations require corrections due to the velocity-slip and temperature-jump. Total algorithm of solution includes three steps: the first step is to solve Eq. (10) and (11). The second step is to solve first order equations and the third step is to solve the second order equations. The SIMPLE algorithm is used for each step. The final solution is the summation of  $U_0, U_1$  and  $U_2$ . A three-part computer program has been provided for solving the three set of discretized equations. A uniform  $300 \times 50$  staggered grid is employed for the present study. The boundary conditions at the channel inlet are:

$$\begin{aligned} u(y)|_{x=0} &= u_0(y)|_{x=0} = u_{in} \\ u_1(y)|_{x=0} &= u_2(y)|_{x=0} = 0 \\ T(y)|_{x=0} &= T_0(y)|_{x=0} = T_{in} \\ T_1(y)|_{x=0} &= T_2(y)|_{x=0} = 0 \end{aligned} \quad (10)$$

#### 4. ANALYTIC SOLUTIONS for FULLY DEVELOPED FLOW in CHANNEL

##### 4.1. Poiseuille Number using Second Order Model

At high Knudsen number, no-slip boundary condition is not a good assumption and slip boundary conditions must be used. For isothermal flows with tangential momentum accommodation coefficient  $\sigma_v = 1$ , for analytical solution we use the general second-order slip condition with the following dimensionless form (Karniadakis and Beskok (2004)):

$$U_s - U_w = C_1 Kn \left( \frac{\partial U}{\partial n} \right) - C_2 Kn^2 \left( \frac{\partial^2 U}{\partial n^2} \right) \quad (11)$$

The  $C_1$  and  $C_2$  are the slip constant coefficients. Different researcher developed this coefficients and in Table 1 some of them shown. More information is available in (Karniadakis and Beskok (2004)). The analytical slip velocity profile is obtained using momentum equation and the above slip model as follows:

$$u(y) = \frac{-6u_m}{\left[ 1 + 6 \frac{2-\sigma_v}{\sigma_v} (C_1 Kn + 2C_2 Kn^2) \right]} \times \left[ \left( \frac{y}{H} \right)^2 - \left( \frac{y}{H} \right) - \frac{2-\sigma_v}{\sigma_v} (C_1 Kn + 2C_2 Kn^2) \right] \quad (12)$$

Poiseuille number for fully developed flow is:

$$Po = Cf . Re = \frac{24}{(1 + 6C_1 Kn + 12C_2 Kn^2)} \quad (13)$$

$C_f$  is wall friction coefficient.

**Table 1 Coefficients for slip models (Karniadakis and Beskok (2004))**

Author(s)	$C_1$	$C_2$
Cercignani (Cercignani and Daneri 1963)	1.1466	0.9756
Revised Cercignani (Hadjiconstantinou 2003)	1.1466	0.647
Deissler (1964)	1	9/8
Hisa and Domoto (1983)	1	0.5
Schamberg (1947)	1	5π/12
Maxwell (Kennard 1938)	1	0
General form	1	-0.5

##### 4.2 Analytical Solution using the Perturbation Methods for the Fully Developed Flow

For the fully developed flow,  $v=0$ ,  $u=u(y)$  and  $P=P(x)$ . Therefore:

$$\begin{aligned} v_0 &= v_1 = v_2 = 0 \\ u_0 &= u_0(y), u_1 = u_1(y), u_2 = u_2(y), \dots \\ P_0 &= P_0(x), P_1 = P_1(x), P_2 = P_2(x), \dots \end{aligned} \quad (14)$$

Hence, different orders of tangential momentum equations are solved with the corresponding boundary conditions. For incompressible flow, slip does not change the flow rate. That is:

$$\dot{m} = \dot{m}_0, \dot{m}_1 = \dot{m}_2 = 0 \quad (15)$$

For fully developed region we solve momentum equations using perturbation expansion for every order of  $Kn$ , so the zeroth order of velocity and its corrections become:

$$\begin{aligned} u_0(y) &= -6u_m \left[ \left( \frac{y}{H} \right)^2 - \left( \frac{y}{H} \right) \right] \\ u_i(y) &= \left( -6 \frac{2-\sigma_v}{\sigma_v} \right)^{i-1} \times \left( i - 1 + 6 \frac{2-\sigma_v}{\sigma_v} \right) \\ &\quad \times u_m \left\{ 6 \left[ \left( \frac{y}{H} \right)^2 - \left( \frac{y}{H} \right) \right] + 1 \right\} \quad i \geq 1 \end{aligned} \quad (16)$$

$i$  is level or order number in perturbation expansion. The final slip velocity profile is obtained by substituting the Eq. (16) into the perturbation expansion of the velocity:

$$\begin{aligned} u(y) &= \sum_{i=0}^n u_i(y) (Kn)^i \\ &= \left( \frac{-6u_m}{\left[ 1 + 6 \frac{2-\sigma_v}{\sigma_v} (Kn - Kn^2) \right]} \right) \\ &\quad \times \left[ \left( \frac{y}{H} \right)^2 - \left( \frac{y}{H} \right) - \frac{2-\sigma_v}{\sigma_v} (Kn - Kn^2) \right] \end{aligned} \quad (17)$$

We use  $C_1$  and  $C_2$  for investigate effects of this coefficients on the analytical solution of Perturbation Method and compare with results of other researcher. If we use Eq.(17) to obtain Poiseuille number, the result is Eq.(13) with  $C_f=1$  and  $C_2=-0.5$ .

#### 5. NUMERICAL RESULTS AND DISCUSSION

To assure that each numerical result is sufficiently accurate, grid resolution studies have been performed for each  $Po$  and  $Nu$ . Fully developed  $Nu$  and  $Po$  number for  $Re = 1$ ,  $Pr = 0.7$  and  $Kn = 0.06$ , obtained from different grids, are shown in Table 2. For these results we used slip-coefficients that proposed by Hisa and Domoto (Karniadakis and Beskok (2004)). As shown in Table 2, a grid with  $300 \times 50$  resolution, is suitable, thus the following results are based on this grid size.

**Table 2. Grid study results**

Grid resolution	$Nu$	$Po$
<b>200 × 20</b>	6.193	17.629
<b>300 × 30</b>	6.218	17.694
<b>300 × 50</b>	6.236	17.735
<b>400 × 60</b>	6.237	17.737

##### 5.1 Hydrodynamics

###### 5.1.1 Comparison Analytical Solution with Numerical Solution using Perturbation Method

As mentioned and shown in Fig.1, the velocity and temperature profiles are uniform at inlet of the channel. In Fig. 2, Dimensionless form of the no-slip velocity profile and the velocity corrections are compared with the analytical solution at once of the sections that the flow is fully developed .As shown, good agreement is found between the analytical and numerical results. In Fig.3, the slip velocity, no-slip velocity and

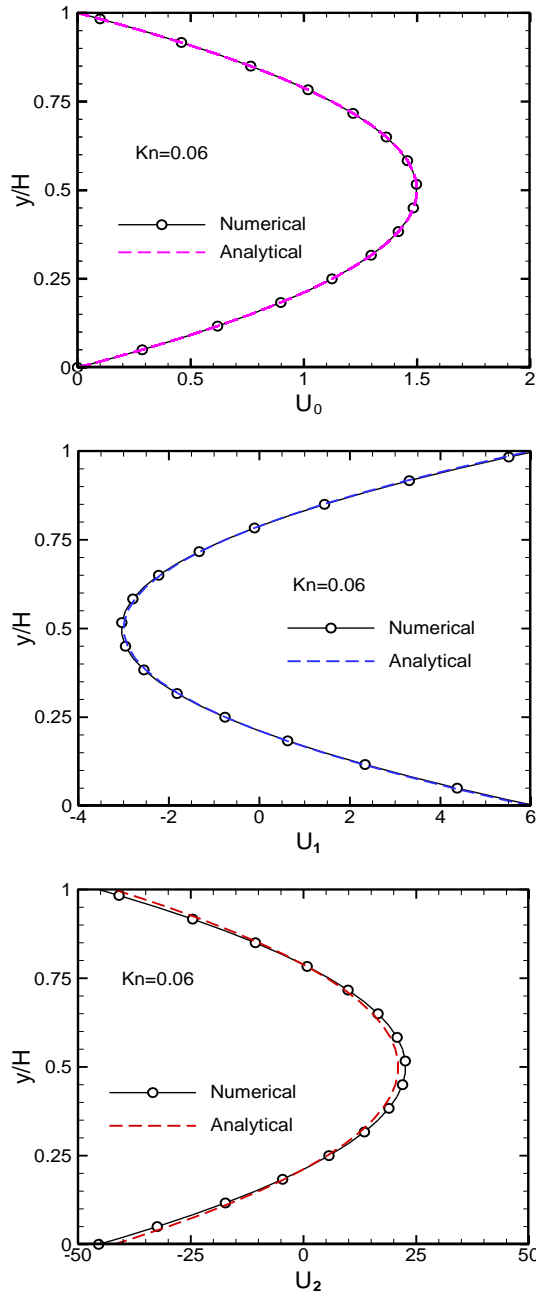


**Fig. 2. Zeroth, first and second order of corrections velocity**

correctional velocities are compared. Zeroth order of velocity or noslip boundary condition velocity profile ( $U_0$ ) is corrected by first order ( $U_1$ ) and second order ( $U_2$ ) corrections to obtain slip velocity profile ( $U$ ).

**5.1.2 Comparison Analytical and Numerical Solution with other Slip Models**

In Fig. 4, the slip and no-slip fully developed velocity profiles obtained by the numerical solution (using perturbation method) and slip velocities obtained by the Eq. (12) are shown. Good agreement is found between the results. For a better comparison between the perturbation method results and the results produced by different slip models, Fig. 5 shows normalized slip

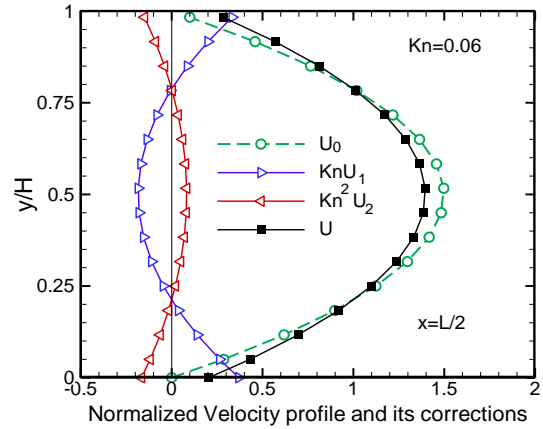


**Fig.3. Fully developed dimensionless slip velocity profile, no-slip velocity and correctional velocities for  $Kn=0.06$ .**

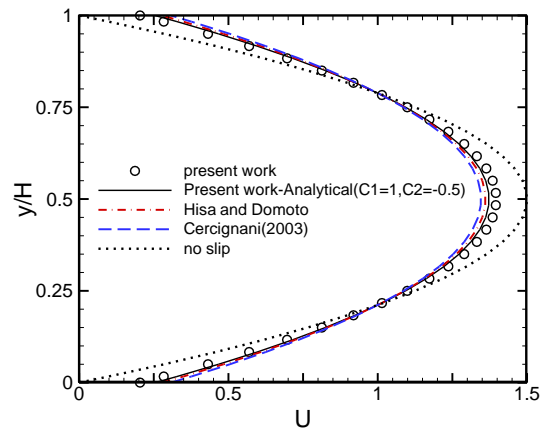


**Fig. 4. Slip and no-slip velocities for  $Kn=0.06$ .**

velocities at the channel walls versus the Knudsen number. If we use only the first order perturbation expansions ( $\varphi = \varphi_0 + Kn \varphi_1$ ), the slip velocity is overpredicted as Knudsen number increased. Also, if we use first and second order perturbation expansions ( $\varphi = \varphi_0 + Kn \varphi_1 + Kn^2 \varphi_2$ ), with  $C_1=1$  and  $C_2=-0.5$  the slip velocity is underpredicted as Knudsen number is increased. However, if we use other slip coefficients such as those proposed by Hisa and Domoto, the model is more reliable compared to other available data. Numerical results of perturbation method deviate from the other results as  $Kn$  is increased. This reveals that more corrections are needed in the perturbation method as  $Kn$  is increased.

In Fig. 6 the result of numerical solution for  $Po$  and analytical solution using Eq. (13) for all slip coefficients that presented in (Karniadakis and Beskok (2004)) are shown. In Fig.6 it is shown that fully developed  $Po$  with Diessler's slip coefficients has a good agreement with corresponding analytical solutions. Also it is seen that  $Po$  decreases with increasing in  $Kn$ .

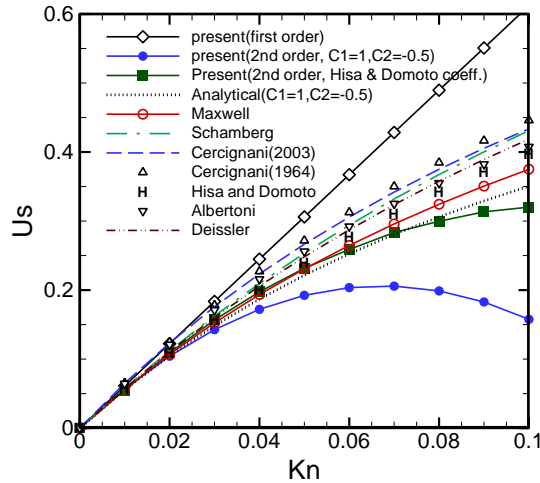


Fig. 5. Dimensionless slip velocity versus  $Kn$  for the Poiseuille flow.

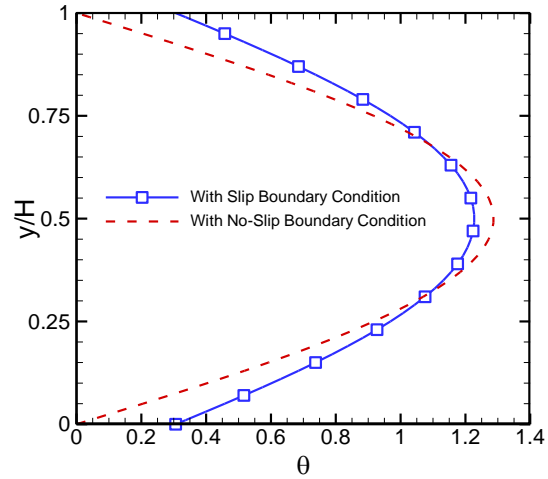


Fig.7. Fully developed dimensionless temperature profiles for slip and no-slip conditions for  $Re = 1$ ,  $Pr = 0.7$  and  $Kn = 0.06$

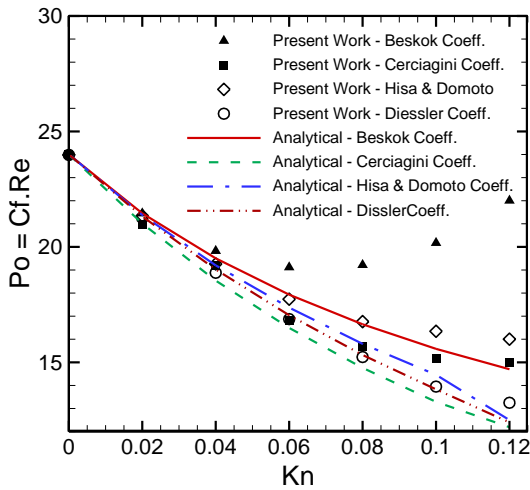


Fig. 6. Variation of fully developed  $Po$  with Knudsen number, for  $Re=1$ .

## 5.2. Heat Transfer

### 5.2.1. Constant Wall Heat Flux Boundary Condition(CWHF)

The zeroth to second order perturbation equations for Constant Wall Heat Flux (CWHF) with  $C_1=1$  and  $C_2= -0.5$  are solved numerically using SIMPLE algorithm. Finally the total temperature ( $T = T_0 + KnT_1 + Kn^2T_2$ ) is calculated. Dimensionless temperature profiles that are defined in Eq. (18) for jump and no-jump conditions are shown in Fig.7. This figure is for a section that the flow is thermally fully developed

$$\theta = \frac{(T_w - T)}{(T_w - T_m)} \quad (18)$$

In Fig.8, Nusselt numbers obtained with different models and for different  $Kn$  are shown and compared with results of Aydinand Avci (2007) and Inman(1964). Then different proposed values for  $C_2$  when  $C_1 = 1$  are

tested. The results are in Fig.8 and Table 3. It is found that for low  $Kn$ , there is a good agreement between  $Nu$  that obtained in present study and  $Nu$  values obtained by Aydinand Avci (2007) and Inman (1964). When  $Kn$  increases, the difference between  $Nu$  obtained in this study and other results is increased. Fig.8 demonstrates that  $Nu$  decreases with increased of  $Kn$ .

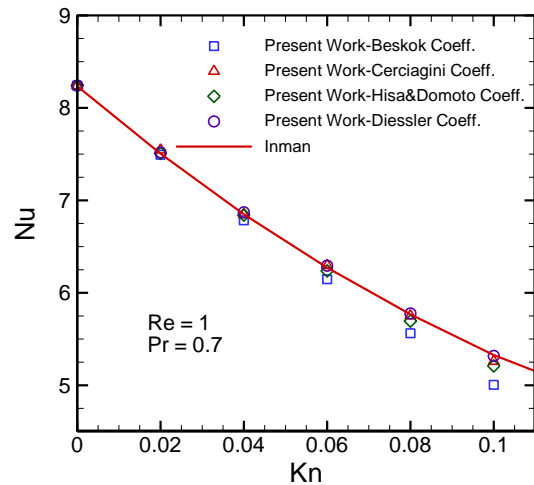
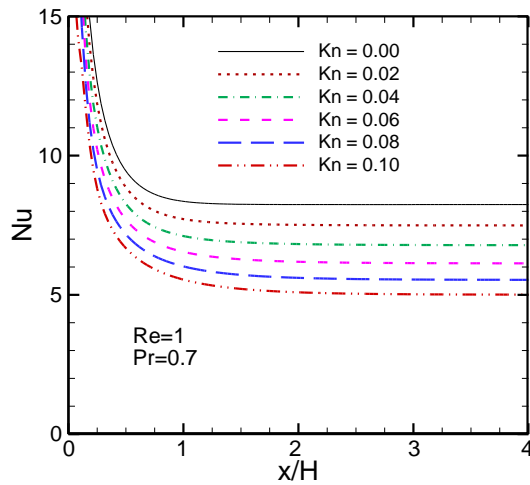


Fig. 8. Variation of fully developed  $Nu$  for CWHF case with  $Kn$  when  $Re = 1$ ,  $Pr = 0.7$

Figure 9 shows that the local Nusselt number decreases when proceeding along the channel. In this figure, it is shown that Nusselt number decreases rapidly at inlet of the channel and then tends to a constant value and this is show developing of flow.  $(\partial T/\partial y)|_w$  And  $(T_w - T_m)$  both decrease rapidly near the inlet of channel but  $(\partial T/\partial y)|_w$  decrease much more rapidly than  $(T_w - T_m)$ , so Nusselt number decreases at first. One can understand from Fig.9 that if  $Kn$  increases then thermal entry length increases. It is noticeable that this Figure is for  $Re = 1$  and we can expect larger thermal entry length in larger Reynolds numbers.

**Table 3. Fully developed Nu values for  $Pr= 0.7, Re = 1$  for the CWHF**

$Kn$	Present work $Nu$ number using Beskok Coeff.	Present work $Nu$ number using Cercignani Coeff. (1964)	Present work $Nu$ number using Hisa&Domoto coeff. (1983)	Present work $Nu$ number using Diessler Coeff. (1964)	$Nu$ number Inman. (1964)	$Nu$ number Aydin. (2007)
0.0	8.241	8.241	8.241	8.241	8.235	8.236
0.02	7.493	7.546	7.508	7.518	7.505	7.5
0.04	6.784	6.847	6.841	6.871	6.849	6.842
0.06	6.147	6.296	6.237	6.293	6.272	6.262
0.08	5.563	5.752	5.694	5.777	5.767	5.756
0.1	5.005	5.260	5.209	5.318	5.327	5.314



**Fig. 9. Axial variation of local  $Nu$  for CWHF case at  $Re = 1, Pr = 0.7$**

**5.2.2 Constant Wall Temperature Solution(CWT)**

Axial variation of temperature is not linear in constant wall temperature (CWT) boundary condition. Therefore axial conduction can be important for CWT cases even if the flow is thermally fully developed. The significance of streamwise conduction is generally established by the magnitude of the flow Peclet number. The Peclet number,  $Pe = Re.Pr$ , represents the ratio of the thermal energy convected to the fluid, to the thermal energy axially conducted within the fluid. A low  $Pe$ , which is common for micro flows, generally indicates that streamwise conduction effects must be considered. Since the  $Pe$  in microchannels as much lower than 100 the effects of axial conduction should be taken into account. In fact we expect that for low  $Pe$ , contribution of axial conduction is considerable compared to convection heat transfer.  $Nu$  is lower than when axial conduction is negligible. The variation of  $Nu$  with  $Kn$  for different values of  $Pe$  for Constant Wall Temperature (CWT) is shown in Fig.10, in this figure it shown that for a fixed  $Pe$ ,  $Nu$  decreases as  $Kn$  is increased. Fig.10 shows effects of  $Pe$  on  $Nu$  in different  $Kn$ . This figure shows good agreement between our numerical results and results presented by Hadjiconstantinou (2003). This figure shows that the  $Nu$  decreases monotonically with increasing  $Kn$  at constant  $Pe$ . The effect of axial heat conduction is to increase the  $Nu$  throughout the slip flow regime. When rarefaction is increasing in  $Kn$ , velocity slip increased so convection heat transfer and  $Nu$  are decreased.

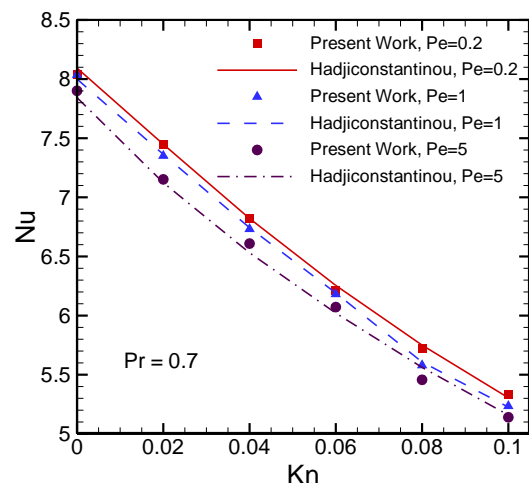


**Fig. 10. Variation of fully developed  $Nu$  number with  $Kn$  number for  $Pe = 0.2, Pe = 1$  and  $Pe = 5$ .**

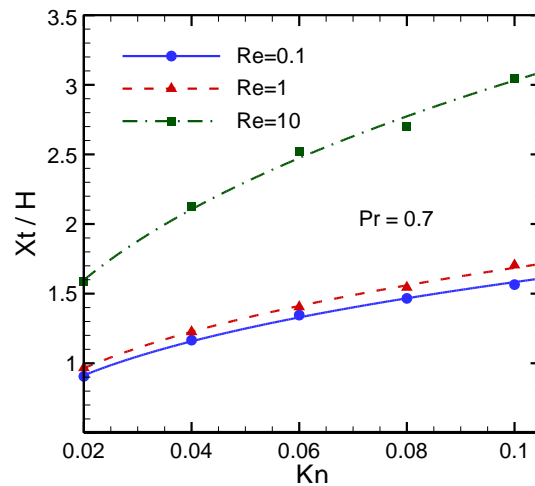


**Fig. 11. Variation of thermal entrance length with Kn number for  $Re = 10, Re = 1, Re = 0.1$  and  $Pr = 0.7$**

Figure 11 shows thermal entrance length for CWT case, with increasing of rarefaction, thermal entrance length is increased. Also when  $Re$  is increased, the thermal entrance length is also increased.

Figure 12 shows dimensionless slip velocity ( $U_s$ ) and temperature jump  $[(T_w - T_s)/(T_m - T_s)]$  in fully developed flow region. This figure show that velocity slip and temperature jump increasing when rarefaction is increased. Also in Fig.13 dimensionless slip velocity and temperature jump for CWT case on wall across the channel are shown for  $Re=1$  and  $Pr=0.7$ .

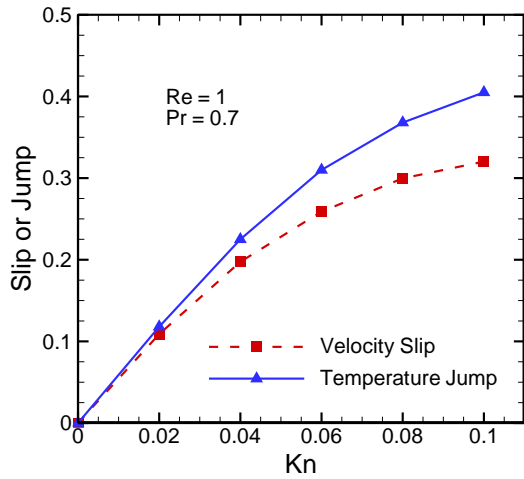


Fig. 12. Velocity slip and temperature jump on wall for  $Re = 1$  and  $Pr = 0.7$

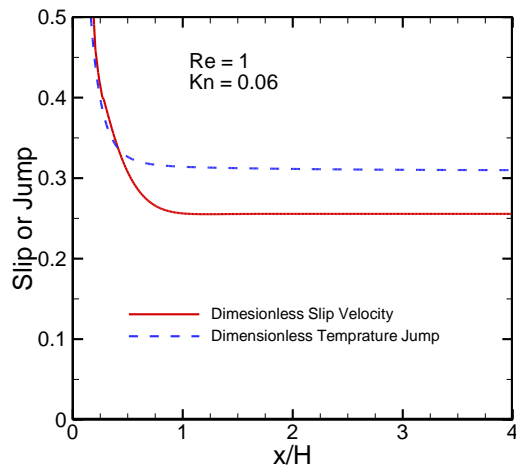


Fig. 13. Velocity slip and temperature jump on wall along the channel length

### 5.3 The Role of the Accommodation Coefficients on Heat Transfer Rate

Momentum and energy transfer between the gas molecules and the surface require specification of interactions between the impinging gas molecules and the surface. A detailed analysis of this is quite complicated and requires complete knowledge of the scattering kernels. The thermal and momentum accommodation coefficients,  $\sigma_T$  and  $\sigma_v$ , are defined by

$$\sigma_T = \frac{dE_i - dE_r}{dE_i - dE_w}, \quad \sigma_v = \frac{\tau_i - \tau_r}{\tau_i - \tau_w} \quad (19)$$

$dE_i$ ,  $dE_r$  denote energy fluxes of incoming and reflected molecules per unit time respectively and  $dE_w$  denotes the energy fluxes if the all incoming molecules had been reemitted with the energy flux corresponding to the surface temperature,  $T_w$  (Karniadakis and Beskok (2004)).

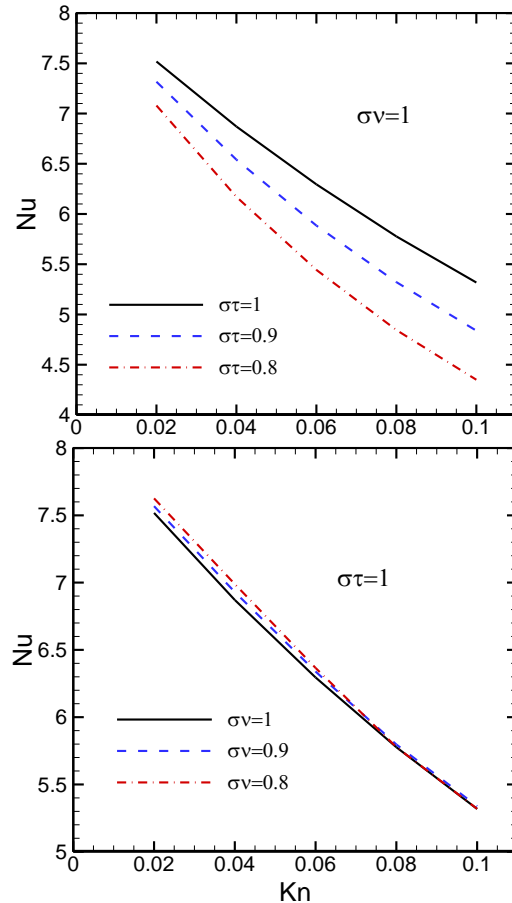


Fig. 14. Variation of  $Nu$  against  $Kn$  for various values of thermal and momentum accommodation coefficients

The effect of accommodation coefficients on heat transfer is shown in Fig.14.  $Nu$  is increasing with increasing in thermal accommodation coefficient and decreasing in momentum accommodation coefficient.

### 5.4 The Effect of Thermal Creep on Flow and Heat Transfer

Thermal creep occurs in gas flows when axial temperature gradients are applied along the channel walls Sone (2002). In channel flows, this boundary treatment induces a tangential creep velocity ( $u_c$ ) in the interior gas close to the walls, such that the gas flows in the direction of the temperature gradient. The following thermal creep  $u_c$  should be added to slip velocity

$$u_c = \frac{3}{4} \frac{\mu}{\rho T_w} \left( \frac{\partial T}{\partial x} \right)_{wall} \quad (20)$$

This case is investigated in present work when constant heat flux (CWHF) boundary condition is applied. The effects of thermal creep flow on fully developed  $Pe$  and  $Nu$  are shown in Fig.15 and Fig.16 for  $Pe = 0.5$  and  $u_c/u_m = +0.25$  (that means thermal creep is in streamwise direction). The results are compared with the available results of Van Rij *et al.* (2007). As shown in Fig.15 and 16, if thermal creep flow has a same direction with streamwise ( $u_c > 0$  or  $(\partial T/\partial x)_w > 0$ ) then it increases Nusselt number and decreases Poiseuille number due to increasing slip in walls.

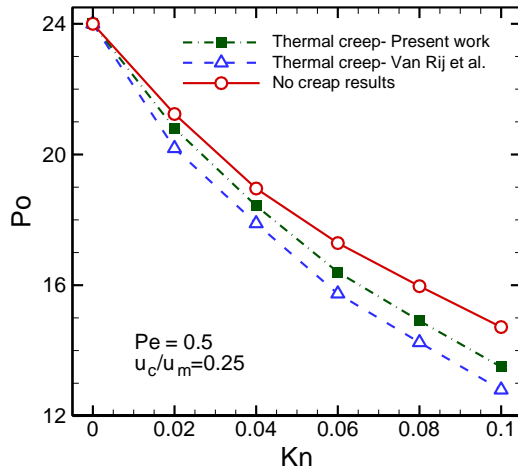


Fig. 15. Effect of thermal creep flow on Poiseuille number for various values of Knudsen number

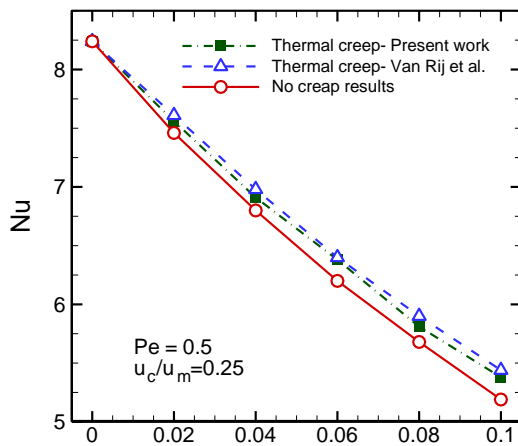


Fig. 16. Effect of thermal creep flow on Nusselt number for various values of Knudsen number

## 6. CONCLUSIONS

In this study slip-flow heat transfer in a laminar, steady state, two-dimensional incompressible flow between parallel plates micro-channel is investigated numerically using perturbation method. Both hydrodynamically and thermally developing flow cases are examined. The Poiseuille and Nusselt numbers for 2-D microchannels with both constant wall heat flux (CWHF) and constant wall temperature (CWT) thermal boundary conditions for the slip flow regime have been numerically investigated. The resulting  $Po$ , and  $Nu$  include the effects of second-order velocity slip and temperature jump boundary conditions. In this study the effects of viscous dissipation and compressibility are neglected. The interactive effect of the rarefaction on Nusselt number has been studied and found that the Nusselt number decreases when rarefaction increases. Also thermal entrance length is investigated and it is found that increasing in  $Re$  or  $Kn$ , leads to increase in thermal entrance length. For CWT case,  $Pe$  has a significant role in heat transfer rate, for low  $Pe$ , thus we should take in to account the effects of axial conduction. Effects of axial conduction increase with

decreasing  $Pe$  and decrease with increasing of rarefaction.

At the end, it is illustrated that when the effect of thermal creep is accounted, if thermal creep has the same direction with streamwise, since the slip velocity at the wall increases, the momentum transfer increases and so Nusselt number increase.

Finally one can conclude that perturbation method is capable to simulate slip flow heat transfer in micro-poiseuille flow

## REFERENCES

- Ameel, T.A., X.M. Wang, R.F. Barron, R.O. Warrington, (1997).Laminar forced convection in a circular tube with constant heat flux and slip flow, *Microscale Thermal Engineering*, 1 (4) 303–320.
- Aydin, O., M. Avci, (2007).Analysis of laminar heat transfer in micro-poiseuille flow, *International Journal of Thermal Science*, 46 30-37.
- Barron, R.F., X. Wang, R.O. Warrington, T. Ameel, (1996).Evaluation of the eigenvalues for the Graetz problem in slip-flow, *Int. Comm. Heat Mass Transfer*, 23 (4) 563–574.
- Barron, R.F., X. Wang, T.A. Ameel, R.O. Warrington, (1997).The Graetz problem extended to slip-flow, *International Journal of Heat and Mass Transfer*, 40 (8) 1817–1823.
- Beskok, A., G.E. Karniadakis, (1994).Simulation of heat and momentum transfer in complex micro-geometries, *Journal of Thermophysics Heat Transfer*, 8 355–370.
- Hadjiconstantinou, N. G., (2003).Comment on Cercignani’s second-order slip coefficient, *Phys. Fluids*, Vol. 15, pp. 2352-2354,
- Hadjiconstantinou, N.G., O., Simek,(2002).Constant-wall-temperature Nusselt Number in Micro and Nano Channels. *Journal of Heat Transfer*, 124, 356-364,
- Inman, R.M.,(1964) Laminar slip flow heat transfer in a parallel-plate channel or a round tube with uniform wall heating, NASA TD-2393.
- Karniadakis, G., A. Beskok, N. Aluru, (2004).*Microflows and Nanoflows Fundamentals and Simulations*, Springer
- Morini, G.L.,(2004).Single-phase convective heat transfer in microchannels: a review of experimental results, *International Journal of Thermal Sciences* 43631–651
- Obot, N.T.,(2002).Toward a better understanding of friction and heat/mass transfer in microchannels— A literature review, *Microscale Thermophysical Engineering*, 6 155–173.

- Palm, B.,(2001).Heat transfer in microchannels, *Microscale Thermophysical Engineering*, 5 155–175.
- Qin, F. H., D. J., Sun, and X. Y., Yin, (2007) Perturbation analysis on gas flow in a straight microchannel, *Physics of fluids*, Vol. 19, pp 027103-14,.
- Sobhan, C.B.,S.V. Garimella, (2001).A comparative analysis of studies on heat transfer and fluid flow in microchannels, *Microscale Thermophysical Engineering*, 5 293–311.
- Sone, Y., (2002).Kinetic Theory and fluid dynamics, Birkhauser, Boston.
- Sparrow, E.M., S.H. Lin, (1962).Laminar heat transfer in tubes under slip-flow conditions, *J. Heat transfer*, 84 (4) 363-369
- Tunc, G. Y., Bayazitoglu,(2001).Heat transfer in microtubes with viscous dissipation, *International Journal of Heat and Mass Transfer*, 44 2395–2403.
- Van Rij, J.V., T., Harman, T. and Ameel, (2007).The effect of creep flow on two-dimensional isoflux microchannels,*International Journal of Thermal Sciences*, 46, 1095-1103.